A Novel Ultra-Wideband Design of Ridged SIW Magic-T

Jia Wang[1, *] and Tianqing Ling[2]

Abstract—In order to obtain a wideband sum-and-difference network, a novel ridged substrate integrated waveguide (RSIW) magic-T is designed. The proposed magic-T is composed of a five-layer RSIW structure. The signal input from the coaxial H-plane port is transmitted to RSIW through a stripline and split into two in-phase and equal signals at the output ports on the top and bottom layers because of the vertically symmetric structure. An E-plane SIW power divider is utilized to realize the E-plane input/output port of the magic-T. A remarkable bandwidth improvement is achieved due to the ridged structure and the wide bandwidth of a ladder-shape stripline optimized by genetic algorithm (GA). Measured results indicate that the magic-T has a fractional bandwidth (FBW) of 78.7% (6.4–14.7 GHz) with return loss better than 18.1 dB and great isolation characteristics.

1. INTRODUCTION

With the continuous development of wireless communication technology, the structure of system has become increasingly complex, and the requirements for the performance and integration of various components are constantly increasing. Magic-T as an important device for microwave and millimeter-wave circuits is widely used in microwave integrated circuits, ultra-wideband reception, and other fields. It is urgent to meet the requirements of ultra-wideband, miniaturization, and high-performance systems [1, 2].

As the wideband matching circuits are difficult to design [3], the FBW of a conventional magic-T is usually limited to 5% to 10% [4, 5]. Using an optimized metal cone profile in the magic-T improved the operating bandwidth to 20% [6]. A narrow band operation is obtained with all general matching configurations [7]. The magic-T consists of microstrip and slotline T-junctions, achieving 40%–50% FBW with good isolation between the sum and difference ports better than 40 dB [8]. The magic-T in [9] using a combination of microstrip-slot transitions and three-line parallel coupled microstrip structure achieved 67% FBW assuming 10 dB of return loss. But the large amount of radiation from the slotline structure causes high insertion losses. The substrate integrated waveguide (SIW) is a new type of transmission line that combines the advantages of rectangular waveguide high-performance and planar transmission lines for easy integration, creating a whole new field for the design of RF microwave circuits. A great number of SIW-based magic-T circuits have been proposed [10–16]. The conventional SIW T/Y junction power dividers used inductive post and large volume to realize equal power distribution [17]. The magic-T based on SIW-slotline transition and SIW T-junction power divider realizes 11.2% (8.4–9.4 GHz) FBW in [18]. By introducing a one-third mode substrate integrated resonator (OTMSIR) and slotline transition, a planar magic-T can be realized, and the bandwidth is 19% (7.4–8.9 GHz) in [4]. These mentioned SIW magic-Ts have a limited bandwidth, which not only use narrow slotline-to-SIW transitions but also add redundant posts to optimize the transition. The conventional SIW T/Y junction H-plane power dividers in [11] require the inductive post and larger volume are to realize equal power distribution.

An SIW magic-T using an E-plane power divider and a slotline transition is proposed in [19], which has a bandwidth of 18% without any redundant posts. In [20], a novel magic-T using a stripline embedded hybrid SIW is designed, which has an FBW of 49.1%. In face of system performance requirements, all these mentioned magic-Ts still do not meet the demands on ultra-wideband and high-performance features. In order to improve the bandwidth of SIW structure, a metal ridged SIW is proposed in [21] and has about 37% enhancement of bandwidth. The RSIW adds ridge capacitance, while reducing the cutoff frequency of TE_{10} allowing the single mode operating bandwidth to be broadened. In [22], by adjusting the width and height of ridge, the single-mode cutoff frequency can be changed, and the relative bandwidth can be expanded. In this paper, a novel broadband RSIW magic-T is designed, to achieve ultra-wideband and meet high-performance system requirement. Due to the wide bandwidth of RSIW structure and a ladder-shape stripline optimized by GA, a definite bandwidth and low-loss improvement of magic-T are realized. All the structures are simulated with HFSS and designed on a dielectric substrate with $\varepsilon_r = 2.94$.

2. DESIGN OF THE RSIW MAGIC-T

2.1. The Design of Ridged Substrate Integrated Waveguide

RSIW is a great substitute for SIW structure to deal with broadband requirements. Inserting a ridge in SIW can widen the mono-modal bandwidth. In order to construct RSIW, SIW is built first based on the equivalent formulas between RW and SIW. The geometry of SIW is shown in Figure 1, where d is the diameter of the post, and p is the distance of two adjacent vias. To prevent the loss between two adjacent vias, the relationship between d and p is [22]:

$$d < 0.2W, \quad d < 0.2\lambda_g, \quad p < 2d \tag{1}$$

The equivalent width W_{eff} and actual w of SIW should satisfy the following formula:

$$W_{eff} = W - 1.08\frac{d^2}{p} + 0.1\frac{d}{W} \tag{2}$$

Figure 2 shows the structure of RSIW. After inserting the ridge, the current in RSIW is mainly concentrated on the edge of the ridge, which could be called current-field edge effect. The effect could be equivalent to edge capacitance C_d, which satisfies the following formula [23]:

$$C_d = \frac{\varepsilon}{\pi}\left[\frac{x^2+1}{x}\cosh^{-1}\left(\frac{1+x^2}{1-x^2} - 2\ln\frac{4}{1-x^2}\right)\right], \quad x = \frac{h}{t} \tag{3}$$

where ε is the dielectric permittivity. The whole capacitance of RSIW consists of double C_d and capacitance of plate capacitor which is proportional to its width and length. The whole capacitance determines the cutoff frequency of TE_{10} mode. In summary, ridge width and gap influence the bandwidth of RSIW structure. In [22], if $W1/(W\text{-}d)$ is between 0.15 and 0.35, the wide bandwidth can be obtained.
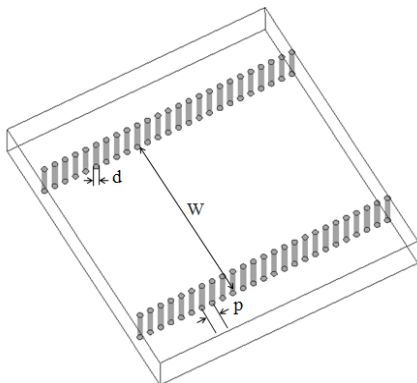

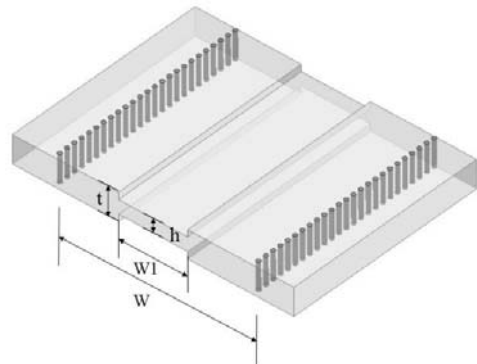**Figure 1.** The structure of SIW.

Figure 2. The structure of RSIW.

Considering that RSIW needs to transit to microstrip, the ridge width could be optimized appropriately. Within a certain range, the bandwidth decreases with an increase in the value of h/t. In consideration of the measurement procedure of $50\,\Omega$ microstrip in Port 1, the total height h cannot be higher than $1.2\,\text{mm}$ on the substrate. In the end, the structure dimensions are $W = 14.4\,\text{mm}$, $W1 = 5.1\,\text{mm}$, $t = 2.2\,\text{mm}$, $h = 1\,\text{mm}$.

2.2. The Ladder-Shape Stripline

The stripline-to-SIW transition has a wider bandwidth than microstrip-to-SIW and slotline-to-SIW transition in [20]. RSIW has the same wave mode as SIW; therefore the transition in SIW can be applied in RSIW structure. Since the characteristic impedance of RSIW has dispersion effects and that of stripline does not change with frequency, the key of transition is to achieve an ideal characteristic impedance matching, in order to transfer signal from the coaxial port (TEM mode) to the RSIW structure (TE_{10} mode).

Four quarter-wavelength impedance transformers are applied to match the RSIW terminal structure. The simulated impedance of RSIW port is 6.5–$9.5\,\Omega$. Using the Chebyshev ladder as the initial value, the widths of four ladder steps are optimized by GA. The initial number of individuals, the maximum number of generations, the crossover probability and the mutation probability are set as 30, 500, 0.9, and 0.05, respectively. After selecting frequency point, 7.0, 7.5, 8.0, 8.5, ..., $14\,\text{GHz}$, the correspondence between the fitness value and S_{44} at each frequency point is as follows:

$$fitness = \begin{cases} 1.0, & S_{44} < -20 \\ 0.8, & -20 \leq S_{44} < -18 \\ 0.5, & -18 \leq S_{44} < -15 \\ 0, & S_{44} \leq -15 \end{cases} \tag{4}$$

The fitness of the transition structure is as in the following function:

$$F = fitness(f_1) + fitness(f_2) + fitness(f_3) + \ldots + fitness(f_{15}) \tag{5}$$

After the optimization by GA, the final selected parameters are $5.7\,\text{mm}$, $3.9\,\text{mm}$, $2\,\text{mm}$, and $0.9\,\text{mm}$. Within the band of the interest, the simulated return loss of Port 4 is greater than $20\,\text{dB}$.

2.3. Wideband RSIW Magic-T

The structural basis of RSIW Magic-T is the ridge substrate integrated waveguide, which achieves a good amplitude and phase consistency by dividing the signal through vertical symmetry of the structure. Figure 3 presents the configuration of the RSIW magic-T. It consists of an E-plane SIW power divider and a coaxial H-plane port. It shows that microstrip Port 1 and coaxial Port 4 are the difference port and sum port, respectively. At the same time, Port 2 and Port 3 are signal dividing arms on the top and bottom layers.

Figure 4 shows the gradation of the E-field distributions, where the principle of RSIW magic-T can be analyzed. For the difference port, when the signal is input from MS Port 1, two equal and out-of-phase signals can be realized by the common ground in the middle and vertical symmetry of the structure at Port 2 and Port 3. When Port 4 is excited, the TEM mode propagates from the coaxial line to the stripline, and a ladder-shape stripline is inserted to transform the TEM mode into the TE_{10} modes in the vertically stacked RSIWs. Because of the vertical and symmetric structure, the signal can be easily divided into two equal and in-phase signals between Port 2 and Port 3.

The ultra-wideband characteristic of the magic-T is determined by two key structures. Firstly, RSIW structure broadens the mono-modal bandwidth by inserting a ridge in SIW, which decreases the cutoff frequency of the dominant mode in magic-T. Secondly, the ladder-shape stripline-to-RSIW transition optimized by GA breaks the limits of the bandwidth of conventional stripline-to-SIW and narrow slotline-to-SIW, helping to widen the bandwidth of magic-T.

Figure 5 presents a planar configuration of the RSIW magic-T, while the dimensions are shown in Table 1. The design of the RSIW magic-T can be divided into following four steps. Firstly, the structural parameters of RSIW determine the operating frequency. The initial value of W is the same as that of the SIW structure in [24], while $W1$ can be optimized considering the microstrip-to-RSIW
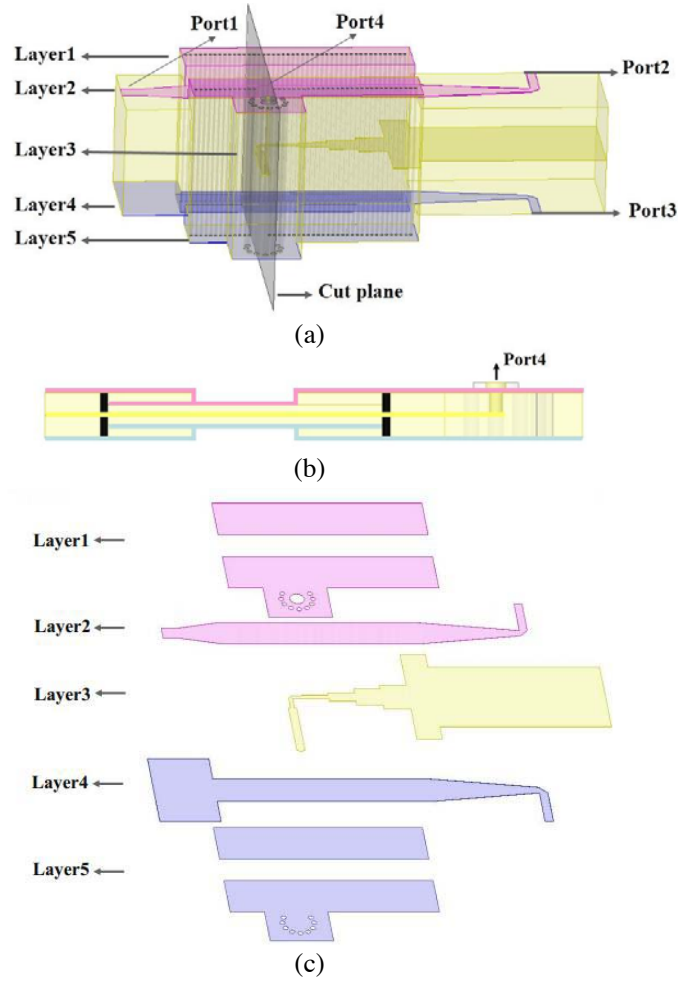
(a)

(b)

(c)

Figure 3. The configuration of the RSIW magic-T. (a) The 3D view; (b) The sectional view; (c) the general view.
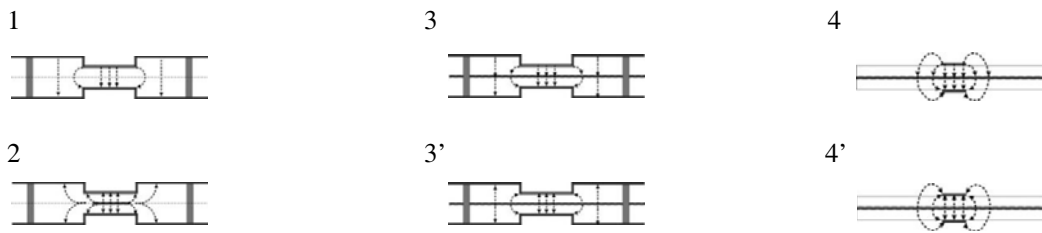

Figure 4. The gradation of the E-field distributions.

transition. Secondly, the parameters of ladder-shape stripline are optimized by GA. The characteristic impedance of stripline at the end is $50\,\Omega$. Thirdly, quasi-coaxial vertical interconnect structure realizes the transition from the stripline to the microstrip line, which consists of 9 posts enclosed in a circle. Distinguished from the stripline-to-mircostrip transition utilized in [20], the proposed stripline-to-coaxial line can reduce the loss of the sum port. In the design, the difference and sum ports are not on the same layer. Hence, the long physical distance can reduce the mutual coupling effect, which highly enhances the isolation. Fourthly, the width of the transition structure between the microstrip and the RSIW is the same as the width of the ridge. Since the electric field near the ridge is quite concentrated and varies greatly with the surrounding structure, the design of the same width of two kinds of transmission lines can reduce loss.
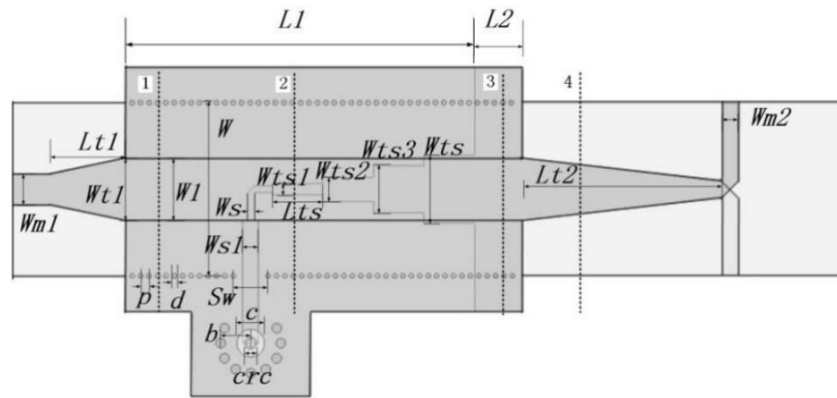
Figure 5. The planar configuration of the RSIW magic-T.

Table 1. Parameters of the structure.

W	14.4 mm	$Lt1$	6.4 mm	Wts	5.7 mm
$W1$	5.1 mm	$Wm1$	2.6 mm	$Wts1$	3.9 mm
d	0.4 mm	$Lt2$	16.6 mm	$Wts2$	2 mm
p	0.7 mm	$Wm2$	1.3 mm	$Wts3$	0.9 mm
$L1$	29 mm	Sw	2.9 mm	Lts	4.2 mm
$L2$	4 mm	crc	0.5 mm	Ws	0.6 mm
c	1.15 mm	b	2.5 mm	$Ws1$	1.3 mm

3. EXPERIMENT AND MEASUREMENT RESULTS

The prototype of RSIW magic-T is fabricated and measured. The magic-T consists of four substrate layers and five copper layers. After completing the circuits of the five copper layers, the two substrate layers are pressed at a high temperature, and the central post of quasi-coaxial structure is drilled. Then all substrate layers and copper layers are pressed in sequence at high temperature. Finally, the through posts from top to bottom of RSIW structure and around posts of the coaxial structure are drilled, then all the holes should be metallized by copper. The entire process is relatively simple, and the use of prepregs to connect the substrate and copper layers can reduce costs. Figure 6 shows the prototype of the fabricated RSIW magic-T. The size of core structure containing the stripline-to-microstrip transition and coaxial port is about $27.4 \times 33\,\text{mm}^2$.

Figure 7 illustrates the results of the simulation and measurement. In the band of 6.4–15 GHz (FBW > 80.4%), the simulated return loss of Port 1 is greater than 20 dB as shown in Figure 7(a),
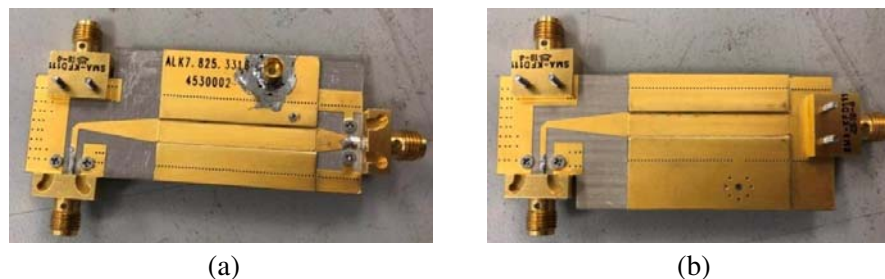

(a)

(b)

Figure 6. Photographs of the fabricated magic-T: (a) Top of magic-T; (b) bottom of magic-T.

while the simulated return loss of Port 4 is better than 20 dB from 6.9 to 14.9 GHz (FBW > 73.4%) shown in Figure 7(b). The simulated return loss of Port 4 is better than 20 dB from 6.9 to 14.9 GHz (FBW > 73.4%). Measured results indicate that the return losses of Port 1 and Port 4 are greater than 18.1 dB and 18.5 dB, respectively. The performance varies greatly because of the machining errors, especially some sensitive dimensions, including the length of the ladder-shape stripline and the gap between multiple layers. Besides, owing to neglect of the SMA connectors in the simulations, errors of measurement results should be also caused by the mismatch between the SMA connectors
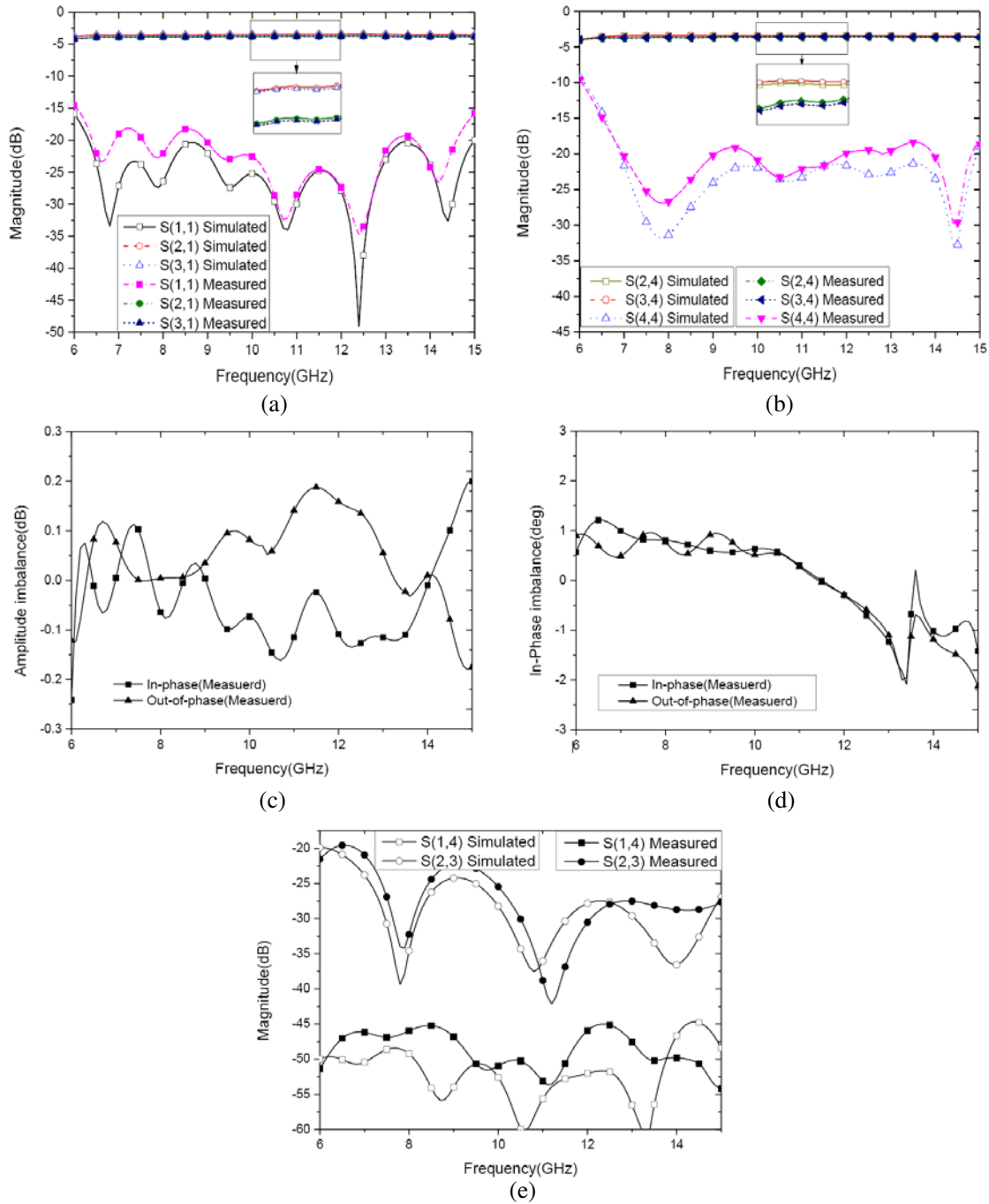

Figure 7. Simulated and measured results of the RSIW magic-T: (a) out-of-phase; (b) in-phase; (c) amplitude imbalance; (d) phase imbalance; (e) isolation.

and microstrip lines. The simulated data and measured results demonstrate that the RSIW magic-T has ultra-wideband and low-loss characteristics. Within the entire bandwidth, the measured phase imbalance and amplitude imbalance for in-phase and out-of-phase are less than $\pm 0.3°$ and $\pm 0.2\,$dB. The differences between amplitude and phase of in-phase and out-of-phase are very small because of the symmetry of the structure. The insertion losses (ILs) of in-phase and out-of-phase are less than $3.65\,$dB and $3.75\,$dB due to IL of microstrip and other transition. Figure 7(d) shows that the measured isolation is greater than $20\,$dB between Port 2 and Port 3, and better than $44\,$dB between Port 1 and Port 4. The performances of the proposed RSIW magic-T and previous magic-Ts in [19, 20] are compared in Table 2, which indicates that this structure achieves lower return loss, wider bandwidth, and more compact structure.

Table 2. Comparisons of performance for different SIW magic-T.

Ref.	FBW	S_{11} (dB)	S_{44} (dB)	S_{41} (dB)	S_{23} (dB)	Size (mm^2)
[19]	17.9% (13.2–15.8 GHz)	12	14.5	< -28	< -12.5	59×38
[20]	49.1% (8.3–13.7 GHz)	15	15	< -40	< -24	18×45
The design	78.7% (6.4–14.7 GHz)	18.1	18.5	< -44	< -20	27.4×33

4. CONCLUSIONS

In this paper, a broadband RSIW magic-T is realized and analyzed. Because of the wideband characteristic of the RSIW structure and a ladder-shape stripline optimized by GA, an improved magic-T with 78.7% bandwidth is realized. The loss is reduced because of the quasi-coaxial vertical interconnect structure and H-plane coaxial port. Besides, the structure is easy to design, and the working frequency band can be adjusted by changing the main mode of RSIW. Because of the broadband and low-loss performance, the magic-T can be used to form UWB sum-and-difference network for beam-forming, signal monitoring, and signal receiving in radar and communication systems. This structure is easy to integrate microwave and millimeter-wave systems, and is conducive to system integration design.

ACKNOWLEDGMENT

REFERENCES

1. Chiang, C.-T. and B.-K. Chung, "Ultra wideband power divider using tapered line," *Progress In Electromagnetics Research*, Vol. 106, 61–73, 2010.

2. Marynowski, W. and J. Mazur, "Investigation of multilayer magic-T configurations using novel microstrip-slotine transitions," *Progress In Electromagnetics Research*, Vol. 129, 91–108, 2012.

3. Khatib, B. Y. E., T. Djerafi, and K. Wu, "Substrate-integrated waveguide vertical interconnects for 3-D integrated circuits," *IEEE Trans. Compon. Packag. Manuf. Technol.*, Vol. 2, 1526–1535, Sep. 2012.

4. Zheng, C. and F. Xu, "A Compact Planar Magic-T Using One-Third Triangular Resonator of Substrate Integrated Waveguide and Slotline Transition," *Microwave Symposium*, 1–4, Jul. 2015.

5. Wu, H. C. and W. B. Dou, "A rigorous analysis and experimental researches of waveguide magic Tee at W band," *Progress In Electromagnetics Research*, Vol. 60, 131–142, 2006.

6. Hwang, K. C., "Design and Optimization of a Broadband Waveguide Magic-T Using a Stepped Conducting Cone," *IEEE Microwave and Wireless Components Letters*, Vol. 19, 539–541, Sep. 2009.

7. Leal-Sevillano, C. A., J. A. Ruiz-Cruz, J. R. Montejo-Garai, et al., "Compact broadband couplers based on the waveguide magic-T junction," *2013 European Microwave Conference*, Oct. 2013.

8. Carl Kim, J. P. and W. S. Park, "Novel configurations of planar multilayer magic-t using microstrip-slotline transitions," *IEEE Transactions on Microwave Theory and Techniques*, Vol. 50, 1683–1688, Jul. 2002.

9. Henin, B. and A. Abbosh, "Wideband hybrid using three-line coupled structure and microstrip-slot transitions," *IEEE Microwave and Wireless Components Letters*, Vol. 23, 335–337, Jul. 2013.

10. He, F. F., K. Wu, W. Hong, L. Han, and X. Chen, "A planar magic-T structure using substrate integrated circuits concept and its mixer applications," *IEEE Trans. Microw. Theory Tech.*, Vol. 59, 72–79, Feb. 2011.

11. Cheng, Y. J. and Y. Fan, "Compact substrate-integrated waveguide bandpass rat-race coupler and its microwave applications," *IET Microw. Antennas Propag.*, Vol. 6, 1000–1006, Jun. 2012.

12. Peng, L., H. Chu, and R. S. Chen, "SIW magic-T with bandpass response," *Electronics Letters*, Vol. 51, 1078–1080, 2015,

13. He, Y. J., D. Y. Mo, Q. S. Wu, and Q. X. Chu, "A Ka-band waveguide magic-T with coplanar arms using ridge-waveguide transition," *IEEE Microwave & Wireless Components Letters*, Vol. 27, 965–967, 2017.

14. Rosenberg, U., M. Salehi, J. Bornemann, and E. Mehrshahi, "A novel frequency-selective power combiner/divider in single-layer substrate integrated waveguide technology," *IEEE Microw. Wirel. Compon. Lett.*, Vol. 23, 406–408, 2013.

15. Huang, J., G. Hua, B. Cao, and F. Ran, "A 34.5 GHz planar magic-T based on coupling slot and substrate integrated waveguide," *2016 IEEE International Conference on Ubiquitous Wireless Broadband (ICUWB)*, 1–3, Oct. 2016.

16. Yang, L., F. Xu, S. Deng, and S. Liu, "A compact planar magic-T using quarter-mode substrate integrated waveguide resonator and slotline coupling transition," *2016 IEEE International Conference on Ubiquitous Wireless Broadband (ICUWB)*, 1–3, Oct. 2016.

17. Germain, S., D. Deslandes, and K. Wu, "Development of substrate integrated waveguide power dividers," *IEEE Electr. Comput. Eng.*, Vol. 3, 1921–1924, May 2003.

18. He, F. F., K. Wu, W. Hong, H. J. Tang, H. B. Zhu, and J. X. Chen, "A planar magic-T using substrate integrated circuits concept," *IEEE Microwave & Wireless Components Letters*, Vol. 18, 386–388, 2008.

19. Feng, W. J., W. Q. Che, and K. Deng, "Compact planar magic-T using *E*-plane substrate integrated waveguide (SIW) power divider and slotline transition," *IEEE Microwave & Wireless Components Letters*, Vol. 20, 331–333, 2010.

20. Zhu, F., W. Hong, J.-X. Chen, and K. Wu, "Design and implementation of a broadband substrate integrated waveguide magic-T," *IEEE Microwave & Wireless Components Letters*, Vol. 22, 630–632, 2012.

21. Li, C., W. Che, P. Russer, and Y. L. Chow, "Propagation and a band broadening effect of planar ridged substrate-intergrated waveguide (RSIW)," *ICMMT2008 Proceedings*, Vol. 2, 467–470, 2008.

22. Li, L., X. Liang, Y. Zhang, X. Wang, et al., "Propagation characteristic of ridge substrate integrated waveguide," *2016 IEEE International Conference on Integrated Circuits and Microsystems*, 195–199, 2016.

23. Somlo, P. I., "The computation of coaxial line step capacitances," *IEEE Trans. Micro. Theory Tech.*, Vol. 15, No. 1, Jan. 1967

24. Sahu, A., R. Mishra, and P. Aaen, "Recent advances in the theory and applications of substrate-integrated waveguides," *International Journal of RF and Microwave Computer-Aided Engineering*, Vol. 26, 129–145, 2016.